ANNALS OF GEOPHYSICS, VOL. 51, N. 1, February 2008

Deep electrical resistivity tomography and geothermal analysis of Bradano foredeep deposits in Venosa area (Southern Italy): preliminary results

Giuseppe Tamburriello (1), Marianna Balasco (2), Enzo Rizzo (2), Paolo Harabaglia (1), Vincenzo Lapenna (2) and Agata Siniscalchi (3)
(1) *DISGG, Università della Basilicata, Campus Macchia Romana, 85100 Potenza, Italy*
(2) *Istituto di Metodologie per l'Analisi Ambientale, CNR, Tito Scalo (PZ), Italy*
(3) *Università degli Studi di Bari, Italy*

Abstract

Geophysical surveys have been carried out to characterize the stratigraphical and structural setting and to better understand the deep water circulation system in the Venosa area (Southern Italy) located in the frontal portion of the southern Appenninic Subduction. In this area there are some deep water wells from which a water conductivity of about 3 mS/cm and a temperature of about 35°C was measured. A deep geoelectrical tomography with dipole-dipole array has been carried out along a profile of 10000 m and an investigation depth of about 900 m. Furthermore a broad band magnetotelluric profile consisting of six stations was performed to infer the resistivity distribution up to some kilometres of depth. The MT profile was almost coincident with the geoelectrical outline. The applied methods allow us to obtain a mutual control and integrated interpretation of the data. The high resolution of the data was the key to reconstruct the structural asset of buried carbonatic horst whose top is located at about 600 m depth. The final results coming from data wells, geothermal analysis and geophysical data, highlighted a horst saturated with salted water and an anomalous local gradient of 60°C/km. The proposed mechanism is that of a mixing of fossil and fresh water circulation system.

Key word *Southern Apennine – geothermal zone – deep electrical resistivity tomography – magnetotelluric survey*

1. Introduction

The Southern Apennine crustal structure is well known, but there are many unknown aspects, among which the position of buried structures near to the accretion prism border. There is a great interest in recognizing the stratigraphical organization of sediments belonging to closure cycle of Foredeep Bradanic and the tectonic structure of the Apulia Platform, that form the Appenninic Orogene Foredeep System. The study area is placed in the Bradanic Deep, a portion of the southern Apennine Foredeep. In particular the investigated area is included between the Vulture volcanic complex in the Southern Apennine and Murge in the Apulia Platform (fig. 1).

Geophysical methods have been effective tools for studying tectonically active areas and reflection seismic and magnetotelluric surveys provide high-resolution images of deep struc-

---

Mailing address: Dr. Enzo Rizzo, Istituto di Metodologie per l'Analisi Ambientale, Consiglio Nazionale delle Ricerche, C.da S.Loja, 85050 Tito (PZ), Italy; e-mail: rizzo@imaa.cnr.it

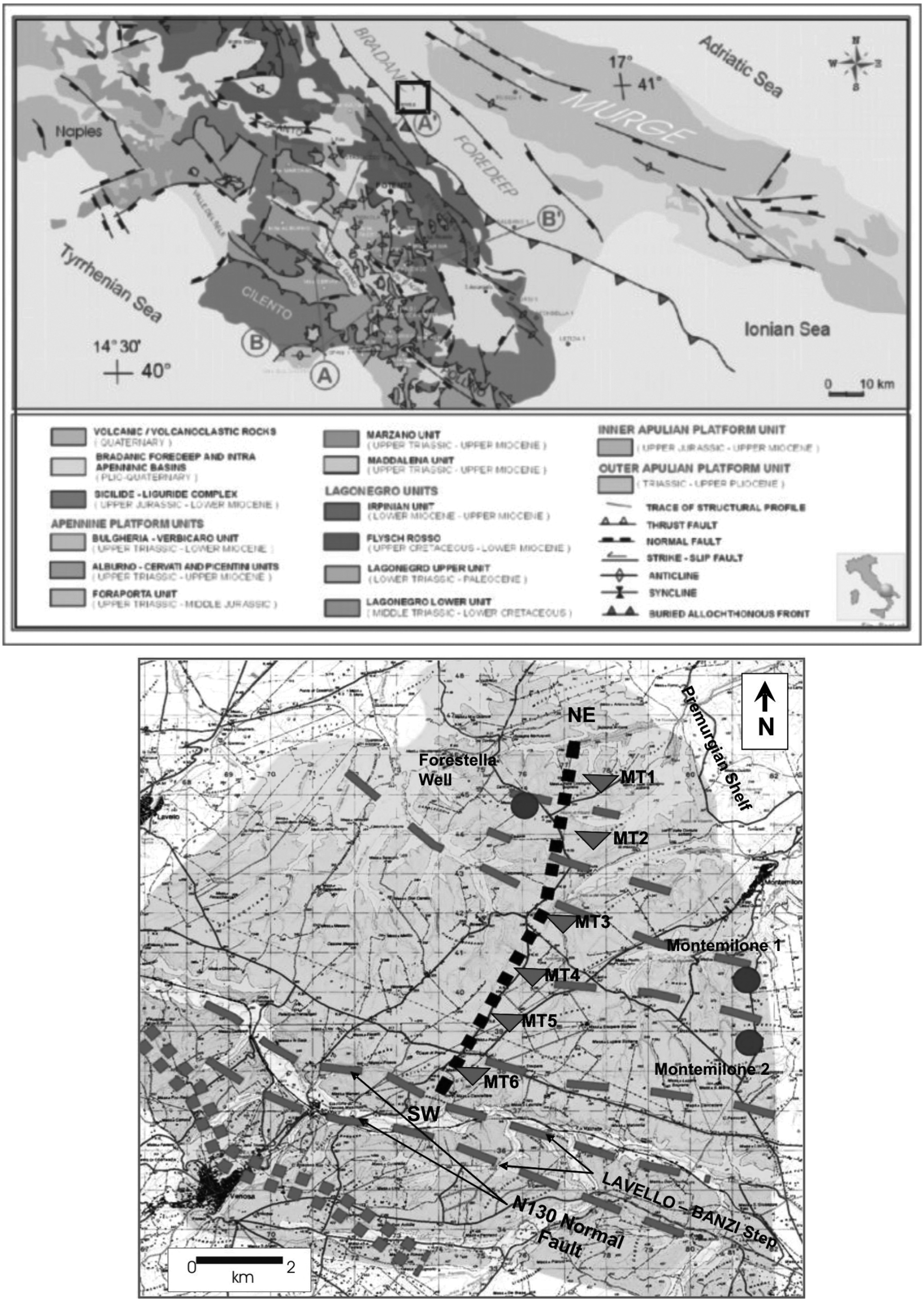

Fig. 1a,b. a) Southern Apennine Structural map (from Menardi Noguera and Rea, 2000). b) Geological survey of the area with the location of geoelectrical survey line (black dots line) and magnetotelluric stations (red triangular shape). The blue circles indicate the wells Montemilone 1 and 2 at East and Forestella well at Nord.

tural systems (Calvert *et al.*, 2001; Hole *et al.*, 2001; Unsworth *et al.*, 1999) giving a major support to geologists. Electrical Resistivity Tomography (ERT) has been widely applied in environmental and engineering geophysics in areas of complex geology (Caputo *et al.*, 2003; Steeples, 2001; Suzuki *et al.*, 2000), even if only few examples of deep ERT (DERT) explorations are reported in the literature (Storz *et al.*, 2000; Colella *et al.*, 2004).

This paper focuses on the analysis of geological and geophysical data compared with borehole stratigraphies to have an image of Apulian buried structures and to understand the deep water circulation system.

The geophysical results, the seismic Bradanic Deep Structural Map (Sella *et al.*, 1988), 3 stratigraphies of AGIP Petroleum drilling wells in the 50' 60' years in the towns of Venosa, Lavello and Montemilone, 2 stratigraphies of fluvial-lacustrine Venosa basin, 2 stratigraphies deep wells of Vulture-Alto-Bradano Consortium help to reconstruct the succession and the lithostratigraphy of the observed area.

2. Geological setting

The Bradanic Deep is the Southern Foredeep of the Plio-Pleistocene's sector and it develops between the Appenninic Chain and the Apulia Foreland (Ricchetti, 1980; Ricchetti and Mongelli, 1980) The latter is flexured and outcrops in Puglia. The bradanic Foredeep is a part of the Southern orogenic System that represents an overthrusting bedding building, coming from the deformation, in a subsequent step, of different paleogeographycal Mesozoic domains. These sedimentary domains are represented by alternation of carbonatic platforms and marine basins that set up a paleogeographical system (D'Argenio *et al.*, 1973).

The Deep external border is represented by «Regional Ramp», built up by a carbonatic substratum area underplating the Apennines (fig. 1). This «ramp» is made up of an inner sector tilt and of an external sector with low tilting to build up a great carbonatic plain named «Premurgiano Shelf» by Pieri *et al.* (1994). This shelf (20-30 Km length) spreads from Cerignola up to Matera and it is located near the Outcropping Apulian Foreland. The two sectors of «shelf» that form the carbonate substratum are displaced by Apennine direction faults to form a huge structural step (Pieri *et al.*, 1996). Pieri *et al.*, 1996 named this great structure the «Lavello-Banzi step». The latest has N130 strike and it is made up of two very closed normal faults, that for more than for 1 km and for a length of 30 km, let down the carbonatic substrate to SW of 1000 m, whose refusal is 500 m each (Sella *et al.*, 1988).

Tropeano *et al.* (1994) recognize in the «ripiano Premurgiano» a complex Horst and Graben structure that reflects the structural characteristic of Outcropping Apulian Foreland. The Bradanic Deep stratigraphical succession is built up of sediments with dissimilar lithologies, facies and thickness. From the bottom to the top this succession is made up of siliceous-clastic sediments related to the carbonatic border, carbonatic sediments related to the eastern border and mixed-class filling basin siliceous-clastic sediments. The silicious-clastic succession is made up of a great thickness argilliferous (clay-silt) sediments (belonging the border basin) and argilliferous silts, marlaceus clay in the axial zone of the basin. In literature these successions are known as Subapennine Clay Formation. The carbonatic successions are made up of biocalcarenitic and biocalciruditic sediments building up a small thickness stratigraphical unit (from 20 m to 70 m) with carbonatic component whose development is closely related to lithologic and shape-structural features of the eastern carbonatic area («regional shelf»). These successions are known as Gravina's Limestone. The filling succession is made up of a high part Bradanic sedimentary regressive cicle with changeable lithostratigraphical features in several zones. These sediments are made up of small thickness silicoclastic sands and conglomerates (30/80 m) traceable back to the transition system (beach-delta) and continental system (river). From a stratigraphy point of view, they are set on Sudapennine Clays with frequently progressive/increasing change and less frequently with erosion contact. Finally the stratigraphical succession is made up of Mesozoic-Cenozoic Limestones of Apulia Platform, Subapennine Clays, Mount Marano's Sands, Irsina's Conglomerate, conglomerates and fluvial-lacustrine sediments, Venosa volcanic sediments, late and current alluvial deposits. The succession ends with Olocenic alluvial deposits made up of sands and gravels with a moderate permeability. Same important structures characterize the Bradanic Deep: in addition to the «Lavello-Banzi step» there are several normal faults located in the surveyed area (fig. 1b).

3. Hydrogeological setting

From drilling wells for irrigating systems it has been possible to verify the presence of two great waterbeds in the considered area. The first is a free surface located from conglomerates and sands, at small depth (50-70 m), caught from shallow Consortium wells and private farming enterprises. These shallow waters are very collected by land owner and because they are not confined and isolated, they are very vulnerable. The second is a great deep water basin, confined, isolated at 500-600 m of depth. This is a very important geothermal basin located in platform limestones underbedding Subapennine Clays considered aquiclude. The collected stratigraphical data allow us to understand the hydro-geological and hydro-chemical features of underground waters in the carbonatic waterbed. Two of deep wells property of Reclaiming Consortium were drilled in the 1990s to catch the carbonatic waterbed underbedding Foredeep clays. With these well stratigraphies, both located in the south of Montemilone, it has been possible to obtain the calcareous depth of -525m in the Montemilone 1 well and -718m in the Montemilone 2 well. The two Montemilone wells (fig. 1b) are aligned and belong the same N-S direction so it is possible to have an approximation of geological formations in the first kilometre of depth.

The water wells data inferred a warm water and a high concentration of chemical elements higher than normal values. These thermal and chemical features indicate that they are a deep salt fluid, which climbs back up from deeper zones due to the convergence of overlapping cover that builds up the Apenninic Chain (Pagliarulo, 1996; Maggiore and Pagliarulo, 1999; Maggiore and Mongelli, 1991; Maggiore, 1996).

4. Methodology: Deep Electrical Resistivity Tomography (DERT)

Electrical resistivity tomography is widely applied in small-scale investigations to solve environmental and engineering problems. Recent improvements in field technology and data processing allow us to apply this method in the large-scale investigations for geological structural studies (Storz *et al.*, 2000; Colella *et al.*, 2004).

A deep geoelectrical tomography with «dipole-dipole» array configuration has been carried out along a profile of 10 km. A dipole-dipole configuration was used where the electric current (I) is sent into the ground via two contiguous electrodes x meters apart, and the potential drop (ΔV) is measured between another two electrodes x meters apart in line with current electrodes. The spacing between the nearest current and potential probes is an integer n times the basic distance x and the maximum number of measurements n depending from the signal-to-noise-ratio of the voltage recordings (Lapenna *et al.*, 1994). In deep geoelectrical explorations a crucial task is the extraction of useful signals from voltage recordings. The voltage signals, generated by the currents injected into the ground by the transmitting stations, are recorded at the receiving remote stations by means of a multivoltmeter connected to a personal computer (acquisition system). The signal-to-noise ratio depends on the distance between the current emitters and receivers and the skill of the statistical tools is related to the duration of voltage recordings. In this work, we carried out the DERT using an electrode spacing of 400 m (x) and a maximum distance between current and potential probes 8/9 n times the basic spacing. In this way, the electrode array geometry allows us to obtain a length of the deep electrical survey of 10000 m, with an exploration depth of about 900 m. We collected

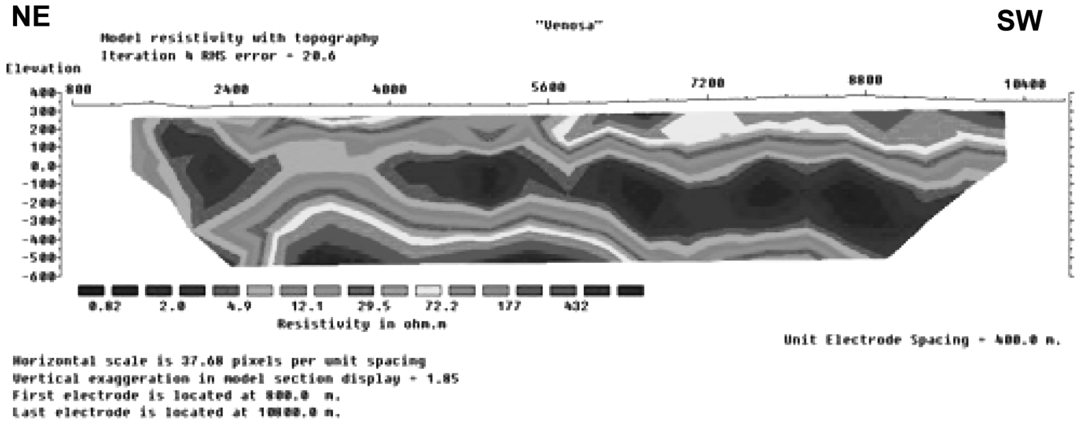

Fig. 2. DERT image with topographic correction.

for each 90 voltage recordings, related to different positions of the electrodes along the profile, current and voltage signals from 5 to 20 min. The voltage signals generated by the artificial current injected into the ground were recorded. The second step consisted in the inversion of the apparent resistivity values obtained during the field survey in real resistivity model of subsoil, using advanced statistical tools for removing the cultural noise and picking out the useful signal. Among the various methods, here we used the inversion algorithm RES2Dinv, a software package by Geotomo Software for determining a 2D resistivity model for the investigated subsoil (Loke, 2003). The Root Mean Squared (RMS) error gives a measure of this difference; in our case it was about 20%.

Figure 2 shows the results of DERT, where a resistivity range from 2 Ω∗m over 4000 Ω∗m is defined. The profile origin has been assumed at the northeastern corner. In this frame it is possible to distinguish three main electrical layers. The first and shallower one is recognizable only from about 5600 m of horizontal displacement from the origin up to the end of the profile and a depth of up to 50 m a.s.l. It yields values in the range 100-700 Ω∗m. Below the shallow resistivity layer, values of resistivity < 30 Ω∗m are observed with a variable thickness between 300 and 700 m. Finally between 2400 m and 6400 m at about depth of –200 m a.s.l., a high resistive zone is observable with values >300 Ω∗m. Such resistivity ranges can be associated with the main lithologies, described previously. The shallow resistivity layer could be associated with conglomerates and sands with a perched groundwater used for irrigation. Such succession is followed by a second more powerful layer constituted by several hundreds metres of Subapennine Clays, associated with the low resistivity layer. The deep high resistive area, could be associated with Apulia Platform's Mesozoic Limestones, displaced by some formal faults, forming a typical Horst geometry.

5. Magnetotelluric investigation

A classical magnetotelluric (MT) sounding requires the measurements of time variations in horizontal components of the naturally electric and magnetic fields on the Earth's surface to obtain the frequency-dependent apparent resistivity curve (Cagniard, 1953). To image the structure of subsoil from the surface down to several kilometres depth, the typical frequency range for such measurements might range from 10^{-4} to 10^{4} Hz.

Our time series data have been analyzed using the Robust Transfer Function Estimation Program for data reduction described in Egbert (1997) to compute the apparent resistivity

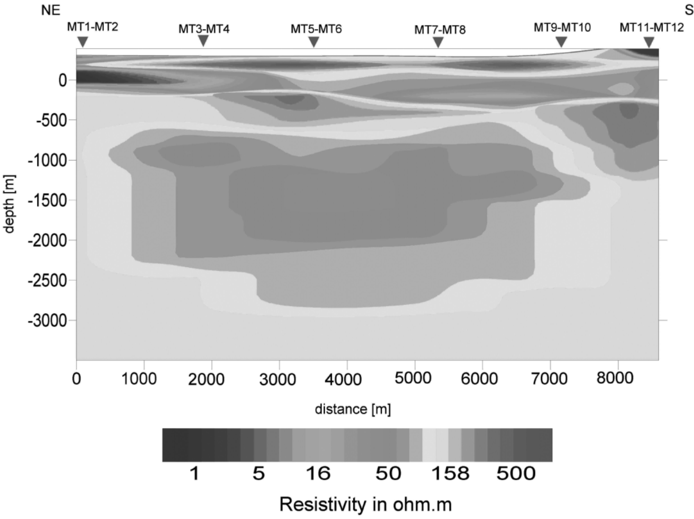

Fig. 3. Resistivity model resulting from the inversion of TM mode.

curves ρ_{xy} and ρ_{yx}, related respectively to the off-diagonal components of impedance tensor Z_{xy} and Z_{yx}. The relationship between two orthogonal component of electric $\overline{E}$ and magnetic $\overline{M}$ fields is given by the following equation (Kaufman and Keller, 1981)

$$\begin{vmatrix} E_x(\omega) \\ E_y(\omega) \end{vmatrix} = \begin{vmatrix} Z_{xx}(\omega) & Z_{xy}(\omega) \\ Z_{yx}(\omega) & Z_{yy}(\omega) \end{vmatrix} \begin{vmatrix} H_x(\omega) \\ H_y(\omega) \end{vmatrix} \qquad (5.1)$$

where ω is the angular frequency, and (E_x, E_y) and (H_x, H_y) represent respectively the electric and magnetic components in an orthogonal reference. The apparent resistivity (ρ) of the ground are defined by the following equations

$$\rho^a_{ij}(\omega) = \frac{1}{\mu_o \omega} \left| Z_{ij}(\omega) \right|^2 \qquad (5.2)$$

where μ_0 is the permeability of the vacuum and Z_{ij} are the complex components of the impedance tensor defined in eq. (2.1), with $i,j = x$ or y.

Where measurements are made in a coordinate system oriented parallel and perpendicular to local geological strike, assuming a 2D electrical structure, the diagonal elements of $|Z|$ should be zero. The off-diagonal elements relating to the electric fields perpendicular and parallel to the geological strike then correspond to impedances associated with TM an TE modes of electromagnetic induction, respectively.

Data shown in this study were collected using MT24-LF receiver (Magnetotelluric 24-bit A/D Low Frequency system) and two induction coils (EMI Inc., BF4) able to detect the electromagnetic natural field (H) in 0.0001-1000 Hz frequency range.

The receiver records 5 channels of data, two components of the magnetic fields and three components of the electric fields. The electric field (E) is measured by a pair of grounded $PbCl_2$ electrodes, distant 100 m apart.

In the present study twelve data sets of apparent resistivity obtained by magnetotelluric recording at six sites, indicated in fig. 1b, have been analyzed.

The frequency of data recording was set to 6.25 Hz for at least ten hours during night-time to reduce the noise level due to artificial e.m. sources, and every night at 2:00 a.m and 4:00 a.m. (GMT) we launched two high frequency sampling acquisition events (1000 Hz) for 30 min, obtaining the apparent resistivity curves in frequency band 0.0061-215 Hz.

In our study E_{x1}, E_{x2} and H_x respectively represent the electric and magnetic field measured in 20N direction (perpendicular to strike of local structure, see fig. 1b) while E_y and H_y the electric and magnetic component along 110N.

Taking into account the direction of the local geological structures MT data were assembled in the two polarization modes (TE and TM): such data exhibit in two soundings a moderate static shift. We use the geoelectrical data to better control this effect (Ingham, 2005). Data were then inverted by using an inversion algorithm (Rodi and Mackie, 2001). Many tests were performed by adopting as *a priori* models of two different types: models with an homogeneous earth resistivity half-space and models based on the resistivity section deduced by the geoelectrical data up to 1 km of depth b.s.l. Topography was taken into account. Even if no substantial difference in the behaviour of the two different model was observed, the best inversion result (the best match with the data) was obtained with the *a priori* geoelectrical model in which the solution converges with a lower rms, giving more reliability on the deeper resistivity anomalies.

Figure 3 shows the resistivity model coming from the inversion procedure of the TM data set. The resistivity values in the electrical model are in logarithmic scale. The electrical image highlights a shallow thin electrical layer (> 300 Ω∗m) up to a low resistivity layer (< 50 Ω∗m), both characterised by a variable thickness. A resistivity zone (> 300 Ω∗m) is located at a depth of about 100 m b.s.l. deepening towards SW. Moreover, the electrical model shows a deep relative low resistivity nucleus at about 1500 m b.s.l.

6 Results and conclusions

Figure 4 sketches a geological section, ob-

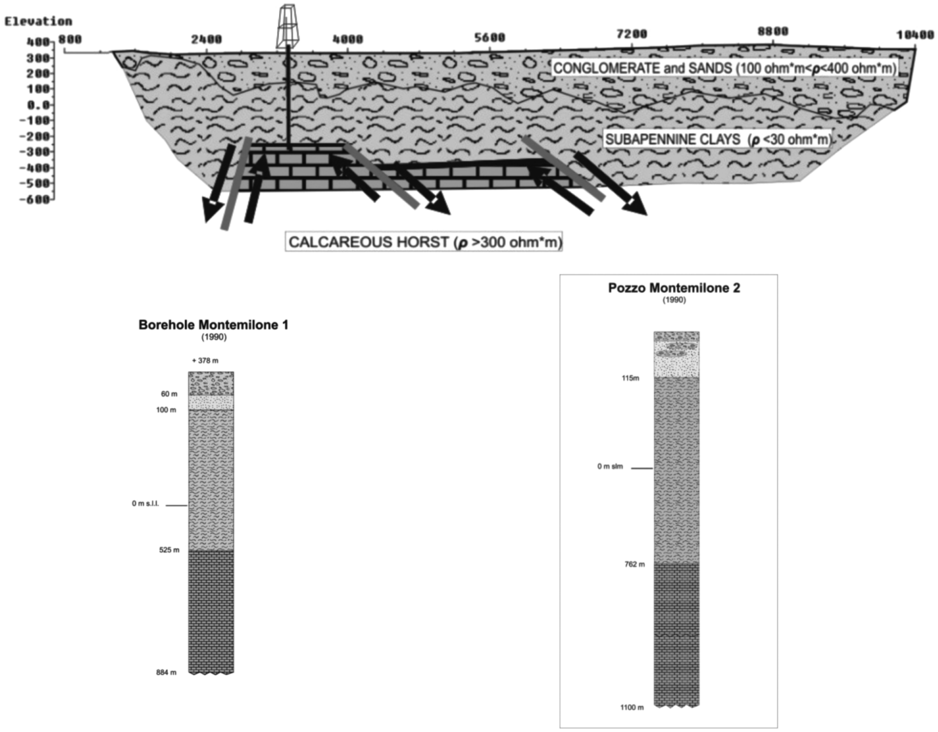

Fig. 4. Geological interpretation interpreted from deep electrical image, shallow MT model and well stratigraphical data of the Montemilone 1 and 2 wells, located at *E* of investigated area.

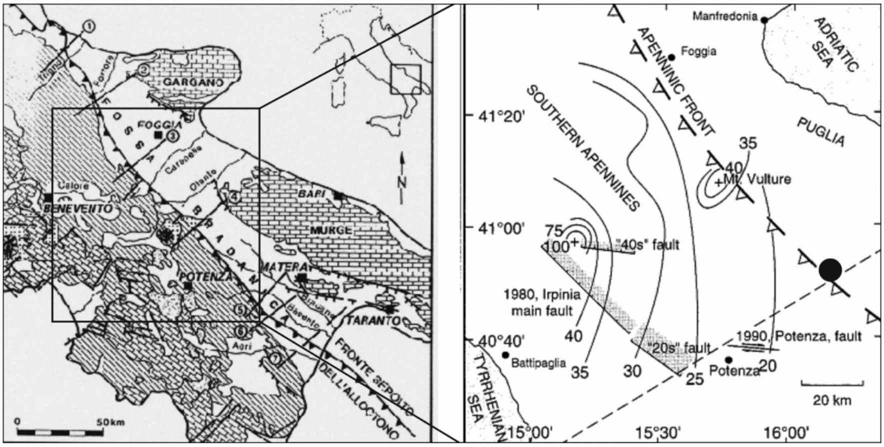

Fig. 5a,b. a) Geological scketch of Southern Italy (from Sella *et al.*, 1988); b) map of the thermal gradient of Southern Appennines in °C/km, the black dot is the investigated area. The «40s» and «20s» represent two faults described in Doglioni *et al.* (1996).

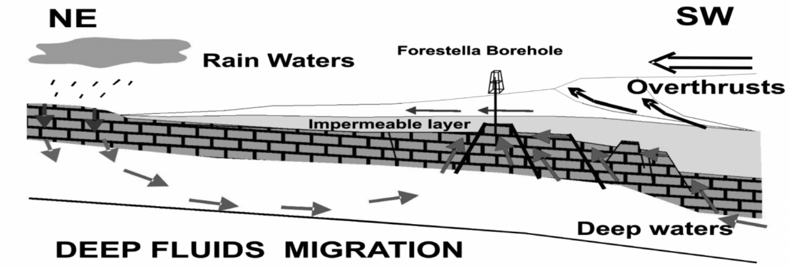

Fig. 6. Schematic section showing the fluids injection and mixing into hydrogeological flow activated by tectonics. The red and blue arrows show the direction of fluids migration.

tained from a geoelectrical image, shallow electrical MT models, geological survey and available stratigraphies of wells (Montemilone 1 and 2).

The geological interpretation image reconstructs the structural asset of a buried carbonatic horst whose top is located at about 600 m beneath the surface.

The Horst, present in the central part of the area, is surely the point in which wells catch the warm and salted water from buried Apulia Platform's limestones. Consequently, this Horst, made up of limestones, is covered by a cap-rock made up of Subappennine Clays. Clays insulate the calcareous horst so that, because of hydrostatic pressure from neighbouring areas, it remains saturated with the warmer water that has been squeezed within. With these considerations it is possible to explain the geothermal anomaly observed in the 560 m deep Forestella well that yields a local geothermal gradient of about 60°C/km, a far higher value than the 20°C/km gradient normal (fig. 5) for the geodynamic setting (Doglioni *et al.*, 1996).

Moreover, the resistivity MT model shows a low resistivity body (~35 Ω∗m, between 700 and 2500 m b.s.l.) which could be associated with a deeper fluid reservoir.

Therefore, the proposed mechanism (fig. 6) is that of a mixing of fossil and fresh water. The fresh fluids (rain waters) come from shallow areas and would be injected into the Foredeep from a hydrogeological high zone into deeper areas with a higher temperature. It is possible that another part of the fluids originates from zones beneath the Apenninic Chain under the action of thrust sheets that probably would produce a pressure forces that move the fluids into permeable layers. It is possible that these waters are formation waters. The overthrust sheets act like a great squeegee that expels fluids in shallow areas (impermeable layers), producing the observed anomalies (Oliver, 1986). When the warm waters arise through discontinuity structures (faults or joints) they could be entrapped in known structures called «traps», that act as reservoirs. In this geological setting the trap is made up of Apulia Platform's limestones, displaced to form a typical Horst structure (observed in the fig. 4) containing fluids heated by the deeper isotherm.

Lastly, this important final result could give the idea to make optimum use of this deep geothermal source as an energy supply.

REFERENCES

CAGNIARD, L. (1953): Basic theory of the magnetotelluric method of geophysical prospecting, *Geophysics*, **18**, p. 605.

CALVERT, A.J., M.A. FISHER and SHIP WORKING GROUP (2001). Imaging the Seattle fault zone with high resolution seismic tomography, *Geophys. Res. Lett.*, **28** (12), 2237-2340.

CAPUTO, R., S. PISCITELLI, A. OLIVETO, E. RIZZO and V. LAPENNA (2003): High-resolution resistivity tomographies in Active Tectonic studies. Examples from the Tyrnavos Basin, Greece, *J. Geodin.*, **36**, 19-35.

COLELLA A., V. LAPENNA and E. RIZZO (2004). High-resolution imaging of the High Agri Valley basin (Southern Italy) with Electrical Resistivity Tomography, *Tectonophysics*, **386**, 29-40.

D'ARGENIO, B., T. PESCATORE and P. SCANDONE (1973): Schema geologico dell'Appennino Meridionale (Campania e Lucania), *Accademia Nazionale dei Lincei*, **182**, 49-72.

DOGLIONI, C., P. HARABAGLIA, G. MARTINELLI, F. MONGELLI and G. ZITO (1996): A geodynamic model of the Southern Apennines, *Terra Nova*, **8**, 540-547

EGBERT, G.D. (1997) Robust multiple-station magnetotelluric data processing, *Geophys J. Int.*, **130**, 475-496.

HOLE, J.A., R.D. CATCHINGS, K.C.ST. CLAIR, M.J. RYMER, D.A. OKAYA and B.J. CAREY (2001). Steep-dip seismic imaging of the shallow San Andreas fault near Parkfield, *Science*, **294**, 1513-1515.

INGHAM, M. (2005). High resolution electrical imaging of fault zones, *Phys. Earth Planet. Int.*, **150**, 93-105.

KAUFMAN, A. and G.V. KELLER (1981): The magnetotelluric sounding method, *Methods Geochem Geophys.*, **15**, 583.

LAPENNA, V., M. MACCHIATO, D. PATELLA, C. SATRIANO, C. SERIO and V. TRAMUTOLI (1994): Statistical analysis of non-stationary voltage recordings in geoelectrical prospecting, *Geophys. Prospect.*, **42** (8), 917-952.

LOKE, M.H. (2003): *RES2Dinv software package by Geotomo Software for determining a 2D resistivity model for the investigated subsoil.*

MAGGIORE, M. (1996): Caratteristiche idrogeologiche e principali differenze idrochimiche delle falde sotterranee del Tavoliere di Puglia, *Mem. Soc. Geol. It.,* **51**, 669-684.

MAGGIORE, M. and F. MONGELLI (1991): Hydrogeothermal model of round water supplì to San Nazario spring (Gargano, Southern Italy), *Quad. Dip. Di Geogr.*, **13**, 307-324.

MAGGIORE, M. and P. PAGLIARULO (1999): Vulnerabilità and main sources of groundwater pollution in the Apulian region (Southern Italy), in *2nd Symposium «Protection of groundwater from pollution and seawater intrusion»*, Bari, 27 settembre-1 Ottobre.

MENARDI NOGUERA, A. and G. REA (2000): Deep structure of the Campanian-Lucanian Arc (Southern Apennine, Italy), *Tectonophysics,* **324**, 239-265

OLIVER, J. (1986): Fluids expelled tectonically from orogenic belts: their role in hydrocarbon migration and other geologic phenomena, *Geology*, **14**, 99-102.

PAGLIARULO, P. (1996): Migrazione di fluidi profondi nel substrato prepliocenico dell'Avanfossa appenninica (bacino pugliese e lucano), *Mem. Soc. Geol. It.*, **51**, 659-668.

PIERI, P., L. SABATO and M. TROPEANO (1994): Evoluzione tettono-sedimentaria della Fossa Bradanica a sud dell'Ofanto nel Pleistocene, in *Guida alle escursioni. Congr. Soc. Geol. It. Bari*, *Quaderni Bibl. Prov. Matera*, **15**, 35-54.

PIERI, P., L. SABATO and M. TROPEANO (1996): Significato geodinamico dei caratteri deposizionali e strutturali della fossa bradanica nel Pleistocene, *Mem. Soc. Geol. It.*, **51**, 501-515.

RICHETTI, G. (1980): Contributo alla conoscenza strutturale della Fossa Bradanica e delle Murge, *Boll. Soc. Geol. It.*, **99**, 421-430.

RICHETTI, G. and F. MONGELLI (1980): Flessione del campo gravimetrico della micropiastra apula, *Boll. Soc. Geol. It.*, **99**, 431-436.

RODI, W. and R.L. MACKIE (2001): Non linear conjugate gradient algorithm for 2D magnetotelluric inversion, *Geophysics*, **6** (1), 174-187.

SELLA, M., C. TURCI and A. RIVA (1988): Sintesi geopetrolifera della fossa bradanica (avanfossa della Catena Appenninica meridionale), *Mem. Soc. Geol. It.*, **41**, 87-107.

STEEPLES, D.W. (2001): Engineering and environmental geophysics at the millenium, *Geophysics*, **66** (1), 31-35.

STORZ, H., W. STORZ and F. JACOBS (2000) Electrical resistivity tomography to investigate geological structures of the earth's upper crust, *Geophys. Prospect.*, **48**, 455-471.

SUZUKI, K., S. TODA, K. KUSUNOKY, Y. FUJIMITSU, T. MOGI and A. JOMORI (2000): Case studies of electrical and electromagnetic methods applied to mapping active faults beneath the tick quaternary, *Eng. Geol.*, **56**, 29-45.

TROPEANO, M., M. MARINO and P. PIERI (1994): Evidenze di tettonica distensiva Plio-Pleistocenica al margine orientale della Fossa Bradanica - L'Horst di Zagarella, *Quaternario*, **7** (2), 597-696.

UUSWORTH, M.J., G. EGBERT and J. BOOKER (1999): High-resolution electromagnetic imaging of the San Andreas Fault in Central California, *J. Geophys. Res.*, **104**, 1131-1150.